HHS Public Access

Author manuscript

Sci Signal. Author manuscript; available in PMC 2019 July 18.

Published in final edited form as:

Sci Signal. ; 12(569): . doi:10.1126/scisignal.aar2124.

Glutathione *S*-transferases promote proinflammatory astrocyte-microglia communication during brain inflammation

Shin-ichi Kano[1,*,†], **Eric Y. Choi**[1,†], **Eisuke Dohi**[1,†], **Swati Agarwal**[1], **Daniel J. Chang**[1], **Ashley M. Wilson**[1], **Brian D. Lo**[1], **Indigo V.L. Rose**[1], **Santiago Gonzalez**[1], **Takashi Imai**[1,2], and **Akira Sawa**[1,3,4,5,*]

[1]Department of Psychiatry and Behavioral Sciences, Johns Hopkins University School of Medicine, Baltimore, MD 21205, USA.

[2]Department of Infectious Diseases and Host Defense, Gunma University Graduate School of Medicine, Maebashi, Gunma 371-8510, Japan.

[3]The Solomon H. Snyder Department of Neuroscience, Johns Hopkins University School of Medicine, Baltimore, MD 21205, USA.

[4]Department of Biomedical Engineering, Johns Hopkins University School of Medicine, Baltimore, MD 21205, USA.

[5]Department of Mental Health, Johns Hopkins University Bloomberg School of Public Health, Baltimore, MD 21205, USA

Abstract

Astrocytes and microglia play critical roles in brain inflammation. Here, we report that glutathione S-transferases (GSTs), particularly GSTM1, promote proinflammatory signaling in astrocytes and contribute to astrocyte-mediated microglia activation during brain inflammation. In vivo, astrocyte-specific knockdown of GSTM1 in the prefrontal cortex attenuated microglia activation in brain inflammation induced by systemic injection of lipopolysaccharides (LPS). Knocking down GSTM1 in astrocytes also attenuated LPS-induced production of the proinflammatory cytokine tumor necrosis factor α (TNF-α) by microglia when the two cell types were co-cultured. In astrocytes, GSTM1 was required for the activation of nuclear factor-κB (NF-κB) and the production of proinflammatory mediators, such as granulocyte-macrophage colony-stimulating factor (GM-CSF) and C-C motif chemokine ligand 2 (CCL2), both of which enhance microglia activation. Our study suggests that GSTs play a proinflammatory role in priming astrocytes and

*Corresponding authors. skano@uab.edu (SK), asawa1@jhmi.edu (AS).
†These authors contributed equally to this work.

Author contributions: S.K. conceived and supervised the project with the guidance of A.S. S.K., E.Y.C., and A.M.W. designed and constructed the virus vectors. E.Y.C., E.D., D.J.C., and A.M.W. prepared and titrated lentiviruses and AAVs. S.K., and E.D. performed stereotactic virus injection experiments. E.Y.C., E.D., S.A., I.V.L.R, S.G., and D.J.C. conducted histology experiments. E.Y.C., E.D., S.A., B.D.L., T.I., and A.M.W. performed cell culture experiments, qRT-PCR analysis, Western blot experiments, and other related experiments.

Competing interests: The authors declare that they have no competing interests.

Data and materials availability: All data needed to evaluate the conclusions in the paper are present in the paper or the Supplementary Materials. AAV-*Gstm1* and *Gstt2* shRNAmir plasmids will be made available upon request and will require a material transfer agreement (MTA).

enhancing microglia activation in a microglia-astrocyte positive feedback loop during brain inflammation.

Introduction

Astrocytes play a critical role in maintaining normal neuronal function by modulating synaptic activity, supporting neuronal survival, and providing metabolic support (1–4). In brain inflammation, astrocytes have been suggested to regulate the activity of microglia, neurons, oligodendrocytes, and immune cells infiltrating from the periphery (4–6). Because both astrocytes and microglia sense immune stimuli and produce inflammatory mediators, it is important to understand the mechanisms by which astrocytes and microglia influence each other's pro-inflammatory activities.

Glutathione (GSH) is a thiol-containing tripeptide and a major antioxidant within cells (7). Decreases in the reduced form (GSH) and increases in the oxidized form (GSSG), are associated with cellular susceptibility to oxidative stress. GSH also influences cellular functions through *S*-glutathionylation, the reversible conjugation of a GSH molecule to reactive cysteine residues in proteins (8, 9). Dysregulation of glutathione metabolism is associated with brain inflammation in various neurological and psychiatric disorders (10–17). It is not clear, however, how the glutathione system influences inflammatory responses at the mechanistic level.

Glutathione *S*-transferases (GSTs) are the enzymes that conjugate GSH to target molecules in phase II of metabolic drug detoxification (18). GSTs are a diverse family of cytosolic, mitochondrial, and microsomal enzymes that prevent cellular damage from the noxious stimuli of xenobiotic metabolites (18–20). GSTs are widely present throughout the body and are particularly abundant in the liver, kidney, and lung (18–20). In addition, some of the alpha, mu, and pi classes of GSTs (GSTA4, GSTM1, and GSTP1, respectively) have been detected in both human and rodent brains (21–23). Notably, a recent study suggested that GSTM1 is one of the most abundant proteins in astrocytes (24).

Accumulating evidence shows that GSTs also influence a wide range of biological mechanisms, such as redox homeostasis, signal transduction, cell proliferation, and cell death (25–27). GSTs exert these regulatory functions by activating or inhibiting their target molecules, such as c-Jun N-terminal kinases (JNK), apoptosis signal-regulating kinase 1 (ASK1), and nuclear factor-κB (NF-κB). through either protein-protein interactions or *S*-glutathionylation (27, 28). The current knowledge about these non-phase II detoxification roles of GSTs, however, is still very limited. In the brain, neuronal GSTP1 has been shown to protect neurons from cell death in an animal model of 1-methyl-4-phenyl-1,2,3,6-tetrahydropyridine (MPTP)-induced degeneration of dopaminergic neurons in the substantia nigra (29). In contrast, the roles of specific GSTs in glial cells have not been well characterized, particularly in vivo.

Genetic studies also suggest that variations in the genes encoding GSTs are involved in neurological and psychiatric disorders with immune dysregulation, such as Parkinson's disease, Alzheimer's disease, multiple sclerosis, schizophrenia, and autism (16, 30–34).

Altered expression of GST activity–related genes has been found to be one of the most drastically changed molecular signatures, together with immune and microglia-related genes, in postmortem brains from patients with late-onset Alzheimer's disease (35). Nevertheless, it has not been shown whether GSTs are involved in the regulation of astrocytes and microglia during brain inflammation.

Here we investigated the role of GST enzymes in astrocytes in a mouse model of brain inflammation. We found that GSTs in astrocytes, particularly GSTM1, were required for microglial activation and TNF-α production in brain inflammation induced by systemic lipopolysaccharide (LPS) administration. Mechanistically, GSTM1 activated NF-κB and induced both pro-inflammatory mediators such as granulocyte-macrophage colony-stimulating factor (GM-CSF, also known as CSF2) and C-C motif chemokine ligand 2 (CCL2) in astrocytes in response to TNF-α and IL-1β. Thus, we propose that GSTs prime the inflammatory responses of astrocytes and enhance the activation of microglia through the secretion of pro-inflammatory mediators by astrocytes.

Results

GSTM1 and GSTT2 are enriched in astrocytes in the mouse brain

Whereas previous studies showed that GSTM1 and GSTP1 proteins are present in the mouse brain (21, 29), region and cell-type specificity of their distribution has not been fully addressed. It has been reported that GSTM1 is one of the most abundant proteins in astrocytes (24). In addition, it is not clear whether other GST enzymes, such as GST theta (GSTT), are also present in the brain. Thus, we examined GSTM1 and GSTT2 in various regions of the mouse brain. As expected, GSTM1 was abundant in the mouse brain, including the cortex, hippocampus, striatum, and cerebellum (Fig. 1A, B and fig. S2A). The amount of GSTM1 in the hippocampus, cerebellum, and the whole brain was nearly equivalent to that in the lung, where GSTM1 has been reported to be abundant (36, 37). GSTT2 also showed a similar pattern, although its abundance in the brain was much lower than that of GSTM1. Immunohistochemical analysis revealed that both GSTM1 and GSTT2 were enriched in astrocytes compared to neurons, oligodendrocytes, and microglia (Fig. 1, C and D, and fig. S1). There was no sex difference in the abundance or distribution of GSTM1 and GSTT2 (Fig. 1, B to D, and fig. S2B). These results suggest that GST enzymes, in particular GSTM1, may regulate astrocyte function in the mouse brain.

GSTM1 and GSTT2 are required in astrocytes for microglia activation in vivo

Because astrocytes play a critical role in brain inflammation, we examined the effect of GSTM1 and GSTT2 knockdown in astrocytes on inflammatory responses in the brain. Systemic administration of LPS is a well-established model to induce brain inflammation and is characterized by the activation of both microglia and astrocytes (38, 39). We used this model to examine the effect of astrocyte-specific knockdown of GSTs on the activation of microglia. We first knocked down GSTM1 by using an adeno-associated virus (AAV) vector encoding green fluorescent protein (GFP) and mir-30-based short hairpin RNA targeting *Gstm1* transcripts (*Gstm1* shRNAmir) downstream of a floxed stop codon (AAV-LSL-GFP-*Gstm1*-shRNAmir) (Fig. S3). The AAV was stereotactically injected into the medial

prefrontal cortex (mPFC) of mice expressing Cre recombinase under the mouse *Gfap* promoter (m*Gfap*-Cre mice) at 3 weeks of age. The expression of GFP was specific for astrocytes (S100β$^+$ cells) in the mPFC of m*Gfap*-Cre mice at 3–4 weeks after the AAV injection (Fig. 2A). We observed no GFP signals in neurons (NeuN$^+$ cells), oligodendrocytes (Olig2$^+$ cells), or microglia (Iba1$^+$ cells). Using this system for knocking down GSTM1 specifically in astrocytes, we injected LPS intraperitoneally and examined the activation status of microglia in the area where GFP$^+$ astrocytes were detected. An AAV virus carrying a non-targeting shRNAmir was used as a negative control. We found that GSTM1 knockdown in astrocytes attenuated the activation of nearby microglia, as judged by morphological changes, at 48 hours after LPS injection (Fig. 2, B to D). We observed no difference in microglia activation at 48 hours after saline injection (fig. S4). The percentage of microglia producing tumor necrosis factor α (TNF-α) after LPS injection was also significantly decreased by GSTM1 knockdown in astrocytes, with substantially weaker TNF-α signals per microglia (Fig. 2, E and F). Microglia activation was similarly attenuated when GSTT2 was knocked down in astrocytes by injection of AAV-LSL-GFP-*Gstt2*-shRNAmir into m*Gfap*-Cre mice (fig. S5). These data show that GSTM1 and GSTT2 in astrocytes were required for the activation of microglia during brain inflammation.

Astrocyte GSTM1 and GSTT2 promote microglia activation in vitro

Microglia and astrocytes can amplify each other's activation by secreting pro-inflammatory mediators (Fig. 3A)(40–43). To understand the mechanisms underlying the effects of GSTM1 knockdown in astrocytes on the activation of microglia, we used a co-culture system of primary mouse astrocytes and immortalized microglial cell lines (BV2 microglia) (Fig. 3B). Purified primary mouse cortical astrocytes (fig. S6) were infected with a lentivirus encoding shRNA targeting *Gstm1* (*Gstm1* shRNA) or control shRNA, and then mixed with BV2 microglia. Then, the mixed cultures as well as monocultures of astrocytes and BV2 cells were challenged with LPS for 6 hours. Under these conditions, LPS induced TNF-α production only from microglia (Fig. 3B). We then compared the effects of GSTM1 knockdown in astrocytes on microglial TNF-α production. Consistent with our in vivo findings, GSTM1 knockdown in astrocytes reduced the amount of TNF-α secretion and mRNA expression at 6 hours after LPS stimulation (Fig. 3, C and D). The induction of transcripts encoding IL-1β (*Il1b*) was also reduced (Fig. 3D). A previous study reported that microglia-derived TNF-α and IL-1β induced pro-inflammatory changes of astrocytes (43). Notably, inhibition of TNF-α and IL-1β signaling by blocking antibodies attenuated the induction of *Tnf, Csf2,* and *Ccl2* mRNAs in our co-cultures (Fig. 3E). Previous studies showed that astrocytes produce GM-CSF (also called CSF2) and CCL2, both of which are potent activators of microglia (40–43), during brain inflammation. Thus, these data support that GSTM1 in astrocytes is required for boosting microglial TNF-α production in a non-cell autonomous manner and indicate the requirement of microglia-derived signals for the induction of astrocyte inflammatory mediators. GSTM1 or GSTT2 overexpression in astrocytes, on the other hand, enhanced the induction of *Tnf* mRNA in co-culture (fig. S7).

GSTM1 promotes the production of inflammatory mediators in astrocytes

To investigate the molecular basis by which GSTM1 regulates astrocyte function during inflammatory responses, we analyzed the effects of GSTM1 knockdown on purified primary

mouse astrocytes. We examined the secretion of GM-CSF and CCL2 from astrocytes in response to the pro-inflammatory cytokines TNF-α and IL-1β. We found that the amount of GM-CSF and CCL2 in the culture supernatants from astrocytes decreased by GSTM1 knockdown (Fig. 4A). We also performed qRT-PCR analysis to examine expression of genes encoding pro- and immunoregulatory mediators. The induction of *Ccl2, Csf1,* and *Csf2* mRNAs, but not *Nos2* mRNA, was impaired by GSTM1 knockdown in astrocytes (Fig. 4B). GSTM1 knockdown also affected the production of immunoregulatory cytokines. *Tgfb1* expression decreased upon GSTM1 knockdown, irrespective of the presence of TNF-α and IL-1β. In contrast, the induction of *Il33* mRNA by TNF-α and IL-1β was enhanced in the absence of GSTM1 (Fig. 4B). These findings showed that GSTM1 regulates the transcription of both pro-inflammatory and immunoregulatory genes in astrocytes.

GSTM1 is required for NF-κB activation downstream of TNF-α and IL-1β signaling in astrocytes

To address the mechanisms underlying altered gene transcription downstream of TNF-α and IL-1β in astrocytes, we analyzed the activation of NF-κB, JNK, and extracellular signal–regulated kinase (ERK), all of which are major mediators of TNF-α and IL-1β signaling, in primary mouse astrocytes. GSTM1 knockdown in astrocytes reduced the phosphorylation of the p65 subunit of NF-κB in response to TNF-α stimulation for 6 hours (Fig. 5, A and B). In contrast, the phosphorylation of JNK, ERK, and the NF-κB inhibitor IkBα were not significantly affected by GSTM1 knockdown at the same time point. Because previous studies reported that pharmacological depletion of GSH dampens TNF-α–induced activation of the NF-κB pathway in primary mouse hepatocytes (44), we next examined the effects of GSH depletion by diethyl maleate (DEM) on TNF-α–induced phosphorylation of p65 in mouse astrocytes. Similar to GSTM1 knockdown, DEM treatment caused reduced p65 phosphorylation in response to TNF-α (Fig. 5C and fig. S8). Thus, these findings indicate that GSTM1 activates NF-κB signaling and induces the expression of pro-inflammatory mediators such as GM-CSF and CCL2, both of which enhance the activation of microglia (Fig. 5D).

Discussion

In this study, we discovered that two GST enzymes, GSTM1 and GSTT2, were required in astrocytes for the enhancement of microglia activation during brain inflammation induced by systemic LPS administration. In addition, GSTM1 promoted the induction of pro-inflammatory mediators in astrocytes such as GM-CSF and CCL2. We further demonstrated that GSTM1 activated the NF-κB pathway in response to TNF-α stimulation in cultured astrocytes. Although further mechanistic studies are necessary, these data have revealed a critical role for GST enzymes in astrocytes in enhancing the activation of microglia in brain inflammation.

Astrocytes and microglia are widely involved in brain inflammatory responses related to infection, autoimmunity, neurodegeneration, injury, and other pathological conditions (1–3, 5, 6). Whereas astrocyte-neuron and microglia-neuron interactions have been extensively studied, less is known about the interactions between astrocytes and microglia in brain

inflammation. Because both of these glial cells sense immune stimuli and produce inflammatory mediators, it is important to understand their mutual regulation. Our findings suggest that GSTM1-mediated astrocyte activation is required for boosting microglia activation. At the same time, our data were consistent with prior findings that microglia are the primary cells to sense inflammatory stimuli such as LPS (Fig. 3). Thus, we hypothesize that microglia undergo a two-step activation; first by stimulation through cell autonomous mechanisms of sensing inflammatory stimuli, such as LPS, and second by astrocyte-derived "amplifier" signals such as GM-CSF and CCL2. Accordingly, the interaction of microglia and astrocytes may form a feed-forward loop to facilitate inflammatory responses in the brain. Recent studies have highlighted the role of activated microglia in the functional polarization of astrocytes, such as neurotoxic A1 and neuroprotective A2 astrocytes, in LPS-induced brain inflammation (39). Our study implies that such differentially activated astrocytes may cause differential microglial activation. Further studies to determine the significance of second-step activation of microglia would address this important question.

The mechanisms by which GSTM1 modulates NF-κB activation and gene expression patterns in astrocytes should be further investigated. Although DEM treatment resulted in attenuated NF-κB activation in astrocytes similar to GSTM1 knockdown, a more detailed study would be required to determine whether GSTM1-mediated *S*-glutathionylation enhances NF-κB activation. DEM treatment may cause NF-κB inactivation by mechanisms other than GSH depletion. Future experiments with a mutant GSTM1 lacking glutathione transferase activity may provide further insight into this important question. Thus, further mechanistic studies would determine the role of *S*-glutationylation in astrocyte activation and address whether such GSTM1-mediated mechanisms are present in other brain inflammation models, such as infections, autoimmune diseases, and neurodegeneration.

Although GSTP was previously studied in an animal model of MPTP-induced degeneration of dopaminergic neurons in the substantia nigra (29), it was not clear whether GST enzymes are involved in additional physiological inflammatory conditions beyond xenobiotics-induced neurodegeneration. Our study demonstrated that GSTM1 and GSTT2 were required for LPS-induced brain inflammation unrelated to xenobiotics such as MPTP, adding to the increasing body of work that supports the role of GSTs as endogenous regulators of physiological processes distinct from phase II of drug detoxification (25–27). Our findings are also consistent with recent reports on pro-inflammatory roles of glutathione and protein *S*-glutathionylation (45–47). It is speculated that many proteins are *S*-glutathionylated by GSTs in various mouse and human cells (25–27). The identification of those target proteins will further facilitate our understanding of immunoregulatory mechanisms by diverse GSTs in different tissues and cell types.

An increasing body of evidence suggests that sex difference considerably influences inflammation and microglia function (48, 49). In our study, we did not specifically analyze the impact of sex difference on the role of GSTM1 in astrocyte-microglia interaction, although some experiments, in particular the in vitro cell culture experiments, were conducted with mixed groups of cells from both male and female mice. In the brain expression data, we did not observe any significant difference between male and female for either GSTM1 or GSTT2 (Fig. 1 and fig. S2). Although additional experiments with a larger

sample size are required, there was no clear evidence supporting a sex-related role GSTM1 in astrocyte-microglia interaction during brain inflammation.

Although our in vitro and in vivo findings are consistent with each other, the time course of these experiments is not directly comparable. For the in vitro experiments, cells were challenged with LPS for 6 hours. We chose 48 hours after LPS injection as a time point for in vivo experiments because microglial morphological changes were not clear at earlier time points after LPS injection. Future studies would address whether microglia-astrocyte interaction occurs at earlier time points in the brain after LPS-induced neuroinflammation.

Based on our findings, we propose that GST variations in human populations may dictate individual variations in inflammatory responses or susceptibility to immune pathology associated with various acute and chronic diseases. Despite the publication of numerous genome-wide association studies and exome sequencing studies, there has been no clear strong genetic evidence supporting a role for GST variations in specific diseases. This indicates that GST variations are not associated with specific disease(s) but rather modify individual responses to homeostatic imbalance, such as inflammation, in a wide range of disorders. Because GST enzymes belonging to different classes are distinct in structure (18–20), small molecule inhibitors or activators of specific GST enzymes may be useful as add-on therapeutic agents to modify the outcome of inflammation caused by various diseases.

Materials and Methods

Mice

mGfap^{Cre} *mice* (lines 73.12 and 77.6) and C57BL/6J mice were purchased from the Jackson Laboratory. C57BL/6 timed pregnant female mice for in vitro cell cultures were purchased from Charles River Laboratories or prepared in-house. Mice were housed in specific pathogen–free facilities at the Johns Hopkins University. All the procedures were approved by the Institutional Animal Care and Use Committee of the Johns Hopkins University.

Virus preparation

Lentiviruses (pLKO.1 and pGIPZ viruses) and adeno-associated viruses (AAVs) were prepared following our established protocols (50–52) and their titers were estimated by quantitative PCR (qPCR)-based methods (50, 51, 53). For lentiviruses, pLKO.1-*Gstm1* shRNA lentiviral vectors (#1, TRCN0000103241; #2, TRCN0000103243; #3, TRCN0000103244; #4, TRCN0000103240) were obtained from the RNA consortium (TRC) library via the Hit center at the Johns Hopkins University School of Medicine; control pLKO.1-*Gstm1* shRNA lentiviral vector (#30323) was obtained from Addgene; and pGIPZ-*Gstt2* shRNAmir lentiviral vectors (#1, V2LMM_67055; #2, V2LMM_218573; #3, V3LMM_449685; #4, V3LMM_449688) and control non-silencing (NS) shRNAmir lentiviral vector (RHS4346) were obtained from the Open Biosystems. pHAGE-Gstm1 and pHAGE-Gstt2 were generated by subcloning mouse Gstm1 and Gstt2 cDNAs into pHAGE vectors. For AAVs, AAV-loxP-Stop-loxP (LSL)-GFP-*Gstm1* shRNAmir was generated based on the most efficient shRNA construct (#4) (fig. S2) following the established protocol (54); and AAV-LSL-GFP-*Gstt2* shRNAmir and AAV-LSL-GFP-NS shRNAmir

were generated by shuttling *Gstt2*-shRNAmir (#2) and NS-shRNAmir from pGIPZ lentiviral vectors into AAV-LSL-GFP vectors.

Cell culture

Primary mouse glial cell cultures were prepared from the cortices of postnatal days 2–5 (P2–5) pups of C57BL/6 mice as described previously (55–57). After careful removal of meninges, single cell suspensions were obtained by serial trituration of cerebral cortices with 20G and 26G needles with a 10-ml syringe. Cells were suspended in DMEM/F12 supplemented with 15% FBS and penicillin/streptomycin (all from Thermo Fisher Scientific), and seeded onto T-75 flasks (Corning) pre-coated with poly-D-lysine (PDL, 25 μg/ml) at approximately two brains per flask. Medium was changed on day 3, and every 2–3 days thereafter. If necessary, lentiviral infection was performed with glial cells on day 10 as described below. To enrich astrocytes, oligodendrocyte lineage cells and microglia on the surface of mixed glial cell culture were vigorously shaken off and astrocytes were then collected as negative fractions after MACS sorting with CD11b Microbeads (Miltenyi Biotec). Collected astrocytes were >98% $GFAP^+$ $CD11b^+$ cells (fig. S6). BV2 microglia were maintained in DMEM/F12 supplemented with 15% FBS and penicillin/streptomycin (all from Thermo Fisher Scientific). Astrocyte-microglia co-cultures were prepared by seeding 5×10^5 astrocytes onto PDL-coated 6-well plates and adding 5×10^4 BV2 cells 2 days later. Purified astrocyte cultures were prepared by seeding 5×10^5 astrocytes, immediately after MACS sorting, onto PDL-coated (10 μg/ml) 6-well plates.

Lentiviral infection

Mixed glia culture was passaged on day 9–12 and reseeded at $4–7 \times 10^6$ astrocytes onto PDL-coated T-75 flasks. On the next day, lentiviruses were added to the culture at 1:1 MOI (multiplicity of infection). For pLKO.1 lentiviruses, the virus-infected cells were enriched by antibiotics-based selection (puromycin, 2.5 μg/ml) for 72 h beginning at 72 h post-infection. For pHAGE lentiviruses, infection efficiency was monitored by GFP signals under a fluorescence microscope. Astrocytes were purified as negative fraction with MACS sorting with CD11b Microbeads, and reseeded onto PDL-coated 6-well plates for further experiment.

In vitro cell stimulation

Astrocyte-microglia co-cultures and purified astrocytes were stimulated with 1 μg/ml of LPS (O55B5, Sigma), TNF-α (50 ng/ml) or IL-1β (10 ng/ml) for 6 hours, respectively. For GSH depletion experiments using diethylmaleate (DEM, Santa Cruz Biotechnology), purified astrocytes were treated with serially diluted DEM for 6 hours. Cells and culture sups were immediately harvested at the end of 6-hour incubation for the downstream assays.

Stereotactic surgery and LPS treatment

Mice at P21–28 were anesthetized and placed in the mouse stereotaxic frame (World Precision Instrument: WPI) to secure the cranium. Then, the mice were injected with 250–500 nl of AAV (2.0×10^{10} GC/μl) at the rate of 100–200 nl/min into the medial prefrontal cortex (mPFC) bilaterally using a NanoFil syringe (WPI) with a 35G beveled needle. The

following stereotactic coordinate was used for injection; AP: +1.5 mm; ML: ±0.2 mm; and DV: −1.8 mm from the bregma. Three to four weeks later, LPS (Sigma, O55:B5, 5 mg/kg) was injected intraperitoneally and the brains were harvested 48 hours later.

Immunohistochemistry

Mice were anesthetized and transcardially perfused with ice-cold PBS followed by 4% paraformaldehyde (PFA). Free floating sections (40 μm in thickness) were prepared by a Leica cryostat and, if necessary, antigen retrieval was performed with 10 mM sodium citrate buffer (pH8.5). The sections were then placed in blocking solution (PBS supplemented with 2% Normal Goat Serum, 1% BSA, 0.1% TritonX, 0.05% Tween-20, and 0.05% sodium azide) for 1 h at room temperature and then incubated at 4°C overnight with the following primary antibodies; rabbit anti-Iba1 (1:400, 019–19741, Wako), goat anti-Iba1 (1:400, NB100–1028, Novus Biologicals), chicken anti-GFP (1:5,000, ab13970, Abcam), mouse anti-NeuN (1:200–400, MAB377, EMD Millipore), rabbit anti-S100β (1:400, ab4066, Abcam), mouse anti-Oligo2 (1:400–1,000, MABN50, EMD Millipore), rabbit anti-GSTM1 (1:250, 12412–1-AP, Protein Tech), rabbit anti-GSTT2 (1:250, 17622–1-AP, Protein Tech), and mouse anti-TNF-α (1:200, 52B83, Abcam). After washing with PBS, the sections were further incubated with fluorophore-conjugated secondary antibodies at 1:400 dilution for 2h at room temperature, followed by DAPI staining (1:50,000) for 10 min at room temperature. The sections were mounted on glass slides with Permafluor™ mounting medium or ProLong Diamond antifade mounting medium (Thermo Fisher Scientific). Images were acquired with Zeiss LSM510 and LSM700 confocal microscopes and a Zen software (Zeiss).

Image analysis

For microglial analysis, Z-stack images were analyzed with Image J (NIH). Three images were taken from the coronal sections of mPFC of each mouse stained with anti-Iba1 and anti-TNF-α. (n=8 mice per group). Microglia activation status was categorized into ramified, intermediate, amoeboid, or round based on cell morphology from Iba1 staining. Then, the activation status was categorized as either activated (intermediate, amoeboid, round) or surveying (ramified) as previously described (58). The quantity and percentage of microglia in each category as well as “activated” microglia were reported per each animal. Percentages of TNF-α–positive microglia per total microglia were also calculated with 20x Z-stack images (n=7 mice for control shRNA and n= 8 mice for *Gstm1* shRNA).

Enzyme linked immunosorbent assay (ELISA)

ELISA was performed using Ready-SET-Go!® Kits (eBioscience) for TNF-α, CCL2, and GM-CSF following a standard protocol (59).

Quantitative reverse transcription (qRT)-PCR analysis

qRT-PCR analysis was performed as previously described (16, 59). Total RNA was isolated using RNeasy Plus Micro Kit (Qiagen), and cDNA was synthesized from using Superscript III kit (Invitrogen with oligo$(dT)_{20}$ primers. qPCR was carried out with Maxima SYBR Green/ ROX qPCR Master Mix (Thermo Fisher Scientific) on ABI 7900HT system (Applied Biosystems) and QuantStudio™ 5 (Thermo Fisher Scientific). Gene-specific primer sets

were obtained from PrimerBank (https://pga.mgh.harvard.edu/primerbank) (60) or designed by using Primer-BLAST (https://www.ncbi.nlm.nih.gov/tools/primer-blast). The primer sequences are available in Table S1.

Western Blotting

Cell lysates were prepared with RIPA buffer and separated on NuPAGE Bis-Tris Mini Gels (Life Technologies), followed by the transfer to PVDF membrane (Millipore) following a standard protocol. After blocking in 5% skim milk/PBS-T, membranes were incubated with the primary antibody overnight at 4ºC, and then incubated with the secondary antibody for 1 h at room temperature. Gel images were captured by ImageQuant Las4000 (GE Healthcare) and the intensities of bands were quantified by Quantity One® imaging analysis software (Bio-Rad). For Fig. 1B, GSTM1 abudance in each brain area relative to that in the lung was calculated. For Fig. 5, B and C, the amounts of phosphorylated proteins relative to those of total proteins were calculated. The following primary antibodies were used; p65 (1:1,000, #8242, Cell Signaling), phospho-p65 (1:1,000, #3033, Cell Signaling), JNK (1:1,000, #9252, Cell Signaling), phospho-JNK (1:1,000, #4668, Cell Signaling), Erk1/2 (1:1,000, #4695, Cell Signaling) phospho-Erk1/2 (1:1,000, #4370, Cell Signaling), GSTM1 (1:500, #12412–1-AP, ProteinTech), GSTT2 (1:500, ab53942, Abcam), HA-tag (1:500, #3724, Cell Signaling) and β-Actin (1:2,000, #sc-47778, Santa Cruz).

Statistical analysis

Mann-Whitney test, Student *t*-test, one-way analysis of variance (ANOVA), and two-way ANOVA were used and $p < 0.05$ was considered statistically significant. For multiple testing corrections, Tukey's post-hoc test, Dunnet's post-hoc test, or Sidak's post-hoc test was utilized as indicated in Figure legend and Table S2. All the statistical analysis was performed with GraphPad Prism 7 (GraphPad Software, Inc.). Detailed values for statistical analysis are provided in Table S2.

Constructs

Lentivirus vector encoding mouse *Gstm1* shRNA (pLKO.1-*Gstm1* shRNA-PuroR) was obtained from the RNAi Consortium (TRC) libraries. Lentivirus vector encoding mouse *Gstt2* shRNAmir (pGIPZ-turboGFP-*Gstt2* shRNAmir) was obtained from Open Biosciences (currently ThermoFisher Scientific). Mouse *Gstm1 and Gstt2* cDNA was PCR-cloned from brain lysates and was inserted into the pRK5-HA vector. Lentiviral construct overexpressing HA-tagged cDNA was generated by inserting a blunt-ended EcoRI-BamHI fragment from pRK5-HA-*Gstm1 or Gstt2* vector into pHAGE-CMV-MCS-IZsGreen vector between a blunted site of NotI and a BamHI site. AAV constructs encoding non-silencing control shRNAmir and *Gstt2* shRNAmir under a LoxP-Stop-LoxP (LSL) cassette was generated by inserting a XhoI-blunt-ended MluI fragment from pGIPZ into pAAV-CMV-LSL-GFP-shRNAmir between a XhoI site and a blunt-ended site of EcoRI. AAV construct encoding *Gstm1* shRNAmir was generated by modifying *Gstm1* shRNA sequences into *Gstm1* shRNAmir sequences with a published protocol (52, 54) and inserting the XhoI-*Gstm1* shRNAmir-EcoRI fragment into pAAV-CMV-LSL-GFP shRNAmir between XhoI and EcoRI sites. The sequences of all the constructs were confirmed by conventional Sanger sequencing.

Lentivirus preparation

HEK-293FT cells (Invitrogen) were transfected with lentiviral vectors (pLKO-puro-shRNA, pGIPZ, and pHAGE) and packaging vectors (pMD.2G, psPAX2) by using lipofectamin 3000 (Invitrogen) with a standard protocol. Briefly, culture supernatants were collected at 48 hours post-transfection and ultracentrifuged 25,000 rpm at 4 °C for 2 h to precipitate the virus. Viral pellets were dissolved in PBS and kept frozen at −80ºC until use. Virus titers were estimated by using a quantitative PCR (qPCR)-based method to detect LTR sequences as described previously (53). LTR F: 5'-TGTGTGCCCGTCTGTTGTGT-3', LTR R: 5'-GAGTCCTGCGTCGAGAGAGC-3', LTR Probe : 5'-CAGTGGCGCCCGAACAGGGA-3.'

AAV preparation

AAV-293 cells (Agilent Technologies) were transfected with AAV vectors (pAAV-LStopL-GFP-shRNAmirs) and helper vectors (pAd helper vector and pAAV2/5 packaging vector) following a standard $CaCl_2$ method with some modifications (61). Transfected cells were harvested 48 hours later and lysed by three rounds of freeze-thaw cycles. The lysates were further sonicated and virus-containing fractions were precipitated by adding ammonium sulfate. Then, the viruses were enriched by OptiPrep™ density gradient ultracentrifugation at 60,000 rpm for 1.5 h, followed by concentration of viruses using Amicon Ultra-100 K filter unit (Millipore). Virus titers were estimated using a qPCR-based method to detect ITR sequence as described previously (50). The following primers and probe were used: AAV2 ITR F: 5'-GGAACCCCTAGTGATGGAGTT-3', AAV2 ITR R: 5'-CGGCCTCAGTGAGCGA-3', AAV2 ITR Probe: 5'-CACTCCCTCTCTGCGCGCTCG-3.'

Quantification of GSTM1 and GSTT2 knockdown efficiency in vivo

The abundance of GSTM1/GSTT2 in AAV-infected GFP^+ cells was quantified as follows. First, the outline of a GFP-expressing cell was traced and GSTM1/GSTT2 signal intensities per pixel were averaged across the traced GFP^+ area. Then, the averaged GSTM1/GSTT2 signal intensities were compared between cells expressing control and *Gstm1*/*Gstt2* shRNA.

Measurement of intracellular total GSH

GSH was measured using Glutathione Assay Kit (703002, Cayman Chemicals) according to a manufacturer's instructions. In brief, astrocytes were harvested in MES buffer after 6-hour incubation with DEM, and sonicated to disrupt cellular membrane. Supernatants were incubated with 10% phosphoric acid (MPA) (Sigma) at room temperature for deproteination. Total GSH was detected by measuring the product of glutathionylated DTNB at 415nm with a kinetic method on a UV spectrophotometer. GSH amount was normalized by the protein amount per each sample.

Supplementary Material

Refer to Web version on PubMed Central for supplementary material.

Acknowledgements

We thank Minae Niwa, Sun-Hong Kim, Yian Chen, Luis Cortina, Sharon Chow, Akiho Murata, and Julia See for technical help; Atsushi Kamiya for BV2 microglia cells; Z. J. Huang (Cold Spring Harbor Laboratory) for AAV-LSL-GFP-shRNAmir constructs; and Fengyi Wan for advice.

Funding: This work was made possible by support from the National Institutes of Health (MH093458 and MH113645 to S.K.; MH094268, MH105660, MH092443, and DA040127 to A.S.), RUSK (to A.S.), BBRF (to A.S.), Stanley (to A.S.), Johns Hopkins Medicine Discovery Fund (to S.K.), and the Department of Psychiatry Venture Discovery Fund (to S.K.).

References and Notes

1. Wang DD, Bordey A, The astrocyte odyssey. Prog Neurobiol 86, 342–367 (2008). [PubMed: 18948166]
2. Molofsky AV, Krencik R, Ullian EM, Tsai HH, Deneen B, Richardson WD, Barres BA, Rowitch DH, Astrocytes and disease: a neurodevelopmental perspective. Genes Dev 26, 891–907 (2012). [PubMed: 22549954]
3. Clarke LE, Barres BA, Emerging roles of astrocytes in neural circuit development. Nat Rev Neurosci 14, 311–321 (2013). [PubMed: 23595014]
4. Khakh BS, Sofroniew MV, Diversity of astrocyte functions and phenotypes in neural circuits. Nat Neurosci 18, 942–952 (2015). [PubMed: 26108722]
5. Sofroniew MV, Multiple roles for astrocytes as effectors of cytokines and inflammatory mediators. Neuroscientist 20, 160–172 (2014). [PubMed: 24106265]
6. Ransohoff RM, Brown MA, Innate immunity in the central nervous system. J Clin Invest 122, 1164–1171 (2012). [PubMed: 22466658]
7. Meister A, Anderson ME, Glutathione. Annu Rev Biochem 52, 711–760 (1983). [PubMed: 6137189]
8. Grek CL, Zhang J, Manevich Y, Townsend DM, Tew KD, Causes and consequences of cysteine S-glutathionylation. J Biol Chem 288, 26497–26504 (2013). [PubMed: 23861399]
9. Janssen-Heininger YM, Nolin JD, Hoffman SM, van der Velden JL, Tully JE, Lahue KG, Abdalla ST, Chapman DG, Reynaert NL, van der Vliet A, Anathy V, Emerging mechanisms of glutathione-dependent chemistry in biology and disease. J Cell Biochem 114, 1962–1968 (2013). [PubMed: 23554102]
10. Kulak A, Steullet P, Cabungcal JH, Werge T, Ingason A, Cuenod M, Do KQ, Redox dysregulation in the pathophysiology of schizophrenia and bipolar disorder: insights from animal models. Antioxid Redox Signal 18, 1428–1443 (2013). [PubMed: 22938092]
11. Butterfield DA, Redox signaling in neurodegeneration. Neurobiol Dis 84, 1–3 (2015). [PubMed: 26171987]
12. Miller AH, Haroon E, Felger JC, The Immunology of Behavior-Exploring the Role of the Immune System in Brain Health and Illness. Neuropsychopharmacology 42, 1–4 (2017). [PubMed: 27909328]
13. Wraith DC, Nicholson LB, The adaptive immune system in diseases of the central nervous system. J Clin Invest 122, 1172–1179 (2012). [PubMed: 22466659]
14. Koga M, Serritella AV, Sawa A, Sedlak TW, Implications for reactive oxygen species in schizophrenia pathogenesis. Schizophr Res 176, 52–71 (2016). [PubMed: 26589391]
15. Landek-Salgado MA, Faust TE, Sawa A, Molecular substrates of schizophrenia: homeostatic signaling to connectivity. Mol Psychiatry 21, 10–28 (2016). [PubMed: 26390828]
16. Kano S, Colantuoni C, Han F, Zhou Z, Yuan Q, Wilson A, Takayanagi Y, Lee Y, Rapoport J, Eaton W, Cascella N, Ji H, Goldman D, Sawa A, Genome-wide profiling of multiple histone methylations in olfactory cells: further implications for cellular susceptibility to oxidative stress in schizophrenia. Mol Psychiatry 18, 740–742 (2013). [PubMed: 22925834]
17. Emiliani FE, Sedlak TW, Sawa A, Oxidative stress and schizophrenia: recent breakthroughs from an old story. Curr Opin Psychiatry 27, 185–190 (2014). [PubMed: 24613987]

18. Hayes JD, Flanagan JU, Jowsey IR, Glutathione transferases. Annu Rev Pharmacol Toxicol 45, 51–88 (2005). [PubMed: 15822171]
19. Landi S, Mammalian class theta GST and differential susceptibility to carcinogens: a review. Mutat Res 463, 247–283 (2000). [PubMed: 11018744]
20. Petermann A, Miene C, Schulz-Raffelt G, Palige K, Holzer J, Glei M, Bohmer FD, GSTT2, a phase II gene induced by apple polyphenols, protects colon epithelial cells against genotoxic damage. Mol Nutr Food Res 53, 1245–1253 (2009). [PubMed: 19753610]
21. Beiswanger CM, Diegmann MH, Novak RF, Philbert MA, Graessle TL, Reuhl KR, Lowndes HE, Developmental changes in the cellular distribution of glutathione and glutathione S-transferases in the murine nervous system. Neurotoxicology 16, 425–440 (1995) [PubMed: 8584275]
22. Awasthi YC, Sharma R, Singhal SS, Human glutathione S-transferases. Int J Biochem 26, 295–308 (1994) [PubMed: 8187927]
23. Al Nimer F, Strom M, Lindblom R, Aeinehband S, Bellander BM, Nyengaard JR, Lidman O, Piehl F, Naturally occurring variation in the Glutathione-S-Transferase 4 gene determines neurodegeneration after traumatic brain injury. Antioxid Redox Signal 18, 784–794 (2013). [PubMed: 22881716]
24. Sharma K, Schmitt S, Bergner CG, Tyanova S, Kannaiyan N, Manrique-Hoyos N, Kongi K, Cantuti L, Hanisch UK, Philips MA, Rossner MJ, Mann M, Simons M, Cell type- and brain region-resolved mouse brain proteome. Nat Neurosci 18, 1819–1831 (2015). [PubMed: 26523646]
25. Tew KD, Townsend DM, Glutathione-s-transferases as determinants of cell survival and death. Antioxid Redox Signal 17, 1728–1737 (2012). [PubMed: 22540427]
26. Board PG, Menon D, Glutathione transferases, regulators of cellular metabolism and physiology. Biochim Biophys Acta 1830, 3267–3288 (2013). [PubMed: 23201197]
27. Townsend DM, Tew KD, The role of glutathione-S-transferase in anti-cancer drug resistance. Oncogene 22, 7369–7375 (2003). [PubMed: 14576844]
28. Jones JT, Qian X, van der Velden JL, Chia SB, McMillan DH, Flemer S, Hoffman SM, Lahue KG, Schneider RW, Nolin JD, Anathy V, van der Vliet A, Townsend DM, Tew KD, Janssen-Heininger YM, Glutathione S-transferase pi modulates NF-kappaB activation and pro-inflammatory responses in lung epithelial cells. Redox Biol 8, 375–382 (2016). [PubMed: 27058114]
29. Smeyne M, Boyd J, Raviie Shepherd K, Jiao Y, Pond BB, Hatler M, Wolf R, Henderson C, Smeyne RJ, GSTpi expression mediates dopaminergic neuron sensitivity in experimental parkinsonism. Proc Natl Acad Sci U S A 104, 1977–1982 (2007). [PubMed: 17267597]
30. Rossignol DA, Genuis SJ, Frye RE, Environmental toxicants and autism spectrum disorders: a systematic review. Transl Psychiatry 4, e360 (2014). [PubMed: 24518398]
31. Kim SK, Kang SW, Chung JH, Park HJ, Cho KB, Park MS, Genetic Polymorphisms of Glutathione-Related Enzymes (GSTM1, GSTT1, and GSTP1) and Schizophrenia Risk: A Meta-Analysis. Int J Mol Sci 16, 19602–19611 (2015). [PubMed: 26295386]
32. Rodriguez-Santiago B, Brunet A, Sobrino B, Serra-Juhe C, Flores R, Armengol L, Vilella E, Gabau E, Guitart M, Guillamat R, Martorell L, Valero J, Gutierrez-Zotes A, Labad A, Carracedo A, Estivill X, Perez-Jurado LA, Association of common copy number variants at the glutathione S-transferase genes and rare novel genomic changes with schizophrenia. Mol Psychiatry 15, 1023–1033 (2010). [PubMed: 19528963]
33. Allen M, Zou F, Chai HS, Younkin CS, Miles R, Nair AA, Crook JE, Pankratz VS, Carrasquillo MM, Rowley CN, Nguyen T, Ma L, Malphrus KG, Bisceglio G, Ortolaza AI, Palusak R, Middha S, Maharjan S, Georgescu C, Schultz D, Rakhshan F, Kolbert CP, Jen J, Sando SB, Aasly JO, Barcikowska M, Uitti RJ, Wszolek ZK, Ross OA, Petersen RC, Graff-Radford NR, Dickson DW, Younkin SG, Ertekin-Taner N, Glutathione S-transferase omega genes in Alzheimer and Parkinson disease risk, age-at-diagnosis and brain gene expression: an association study with mechanistic implications. Mol Neurodegener 7, 13 (2012). [PubMed: 22494505]
34. Lee YH, Seo YH, Kim JH, Choi SJ, Ji JD, Song GG, Meta-analysis of associations between MTHFR and GST polymorphisms and susceptibility to multiple sclerosis. Neurol Sci 36, 2089–2096 (2015). [PubMed: 26150166]
35. Zhang B, Gaiteri C, Bodea LG, Wang Z, McElwee J, Podtelezhnikov AA, Zhang C, Xie T, Tran L, Dobrin R, Fluder E, Clurman B, Melquist S, Narayanan M, Suver C, Shah H, Mahajan M, Gillis T,

Mysore J, MacDonald ME, Lamb JR, Bennett DA, Molony C, Stone DJ, Gudnason V, Myers AJ, Schadt EE, Neumann H, Zhu J, Emilsson V, Integrated systems approach identifies genetic nodes and networks in late-onset Alzheimer's disease. Cell 153, 707–720 (2013). [PubMed: 23622250]

36. Knight TR, Choudhuri S, Klaassen CD, Constitutive mRNA expression of various glutathione S-transferase isoforms in different tissues of mice. Toxicol Sci 100, 513–524 (2007). [PubMed: 17890767]
37. Henderson CJ, McLaren AW, Wolf CR, In vivo regulation of human glutathione transferase GSTP by chemopreventive agents. Cancer Res 74, 4378–4387 (2014). [PubMed: 24934809]
38. Burda JE, Sofroniew MV, Reactive gliosis and the multicellular response to CNS damage and disease. Neuron 81, 229–248 (2014). [PubMed: 24462092]
39. Liddelow SA, Guttenplan KA, Clarke LE, Bennett FC, Bohlen CJ, Schirmer L, Bennett ML, Munch AE, Chung WS, Peterson TC, Wilton DK, Frouin A, Napier BA, Panicker N, Kumar M, Buckwalter MS, Rowitch DH, Dawson VL, Dawson TM, Stevens B, Barres BA, Neurotoxic reactive astrocytes are induced by activated microglia. Nature 541, 481–487 (2017). [PubMed: 28099414]
40. Mayo L, Trauger SA, Blain M, Nadeau M, Patel B, Alvarez JI, Mascanfroni ID, Yeste A, Kivisakk P, Kallas K, Ellezam B, Bakshi R, Prat A, Antel JP, Weiner HL, Quintana FJ, Regulation of astrocyte activation by glycolipids drives chronic CNS inflammation. Nat Med 20, 1147–1156 (2014). [PubMed: 25216636]
41. Ponomarev ED, Shriver LP, Maresz K, Pedras-Vasconcelos J, Verthelyi D, Dittel BN, GM-CSF production by autoreactive T cells is required for the activation of microglial cells and the onset of experimental autoimmune encephalomyelitis. J Immunol 178, 39–48 (2007) [PubMed: 17182538]
42. Imai Y, Kohsaka S, Intracellular signaling in M-CSF-induced microglia activation: role of Iba1. Glia 40, 164–174 (2002). [PubMed: 12379904]
43. Saijo K, Winner B, Carson CT, Collier JG, Boyer L, Rosenfeld MG, Gage FH, Glass CK, A Nurr1/CoREST pathway in microglia and astrocytes protects dopaminergic neurons from inflammation-induced death. Cell 137, 47–59 (2009). [PubMed: 19345186]
44. Lou H, Kaplowitz N, Glutathione depletion down-regulates tumor necrosis factor alpha-induced NF-kappaB activity via IkappaB kinase-dependent and -independent mechanisms. J Biol Chem 282, 29470–29481 (2007). [PubMed: 17690092]
45. Tan KS, Lee KO, Low KC, Gamage AM, Liu Y, Tan GY, Koh HQ, Alonso S, Gan YH, Glutathione deficiency in type 2 diabetes impairs cytokine responses and control of intracellular bacteria. J Clin Invest 122, 2289–2300 (2012). [PubMed: 22546856]
46. Salzano S, Checconi P, Hanschmann EM, Lillig CH, Bowler LD, Chan P, Vaudry D, Mengozzi M, Coppo L, Sacre S, Atkuri KR, Sahaf B, Herzenberg LA, Herzenberg LA, Mullen L, Ghezzi P, Linkage of inflammation and oxidative stress via release of glutathionylated peroxiredoxin-2, which acts as a danger signal. Proc Natl Acad Sci U S A 111, 12157–12162 (2014). [PubMed: 25097261]
47. Mak TW, Grusdat M, Duncan GS, Dostert C, Nonnenmacher Y, Cox M, Binsfeld C, Hao Z, Brustle A, Itsumi M, Jager C, Chen Y, Pinkenburg O, Camara B, Ollert M, Bindslev-Jensen C, Vasiliou V, Gorrini C, Lang PA, Lohoff M, Harris IS, Hiller K, Brenner D, Glutathione Primes T Cell Metabolism for Inflammation. Immunity 46, 675–689 (2017). [PubMed: 28423341]
48. McCarthy MM, Sex differences in neuroimmunity as an inherent risk factor. Neuropsychopharmacology, (2018).
49. Markle JG, Fish EN, SeXX matters in immunity. Trends Immunol 35, 97–104 (2014). [PubMed: 24239225]
50. Aurnhammer C, Haase M, Muether N, Hausl M, Rauschhuber C, Huber I, Nitschko H, Busch U, Sing A, Ehrhardt A, Baiker A, Universal real-time PCR for the detection and quantification of adeno-associated virus serotype 2-derived inverted terminal repeat sequences. Hum Gene Ther Methods 23, 18–28 (2012). [PubMed: 22428977]
51. Kano S, Yuan M, Cardarelli RA, Maegawa G, Higurashi N, Gaval-Cruz M, Wilson AM, Tristan C, Kondo MA, Chen Y, Koga M, Obie C, Ishizuka K, Seshadri S, Srivastava R, Kato TA, Horiuchi Y, Sedlak TW, Lee Y, Rapoport JL, Hirose S, Okano H, Valle D, O'Donnell P, Sawa A, Kai M, Clinical utility of neuronal cells directly converted from fibroblasts of patients for neuropsychiatric

disorders: studies of lysosomal storage diseases and channelopathy. Curr Mol Med 15, 138–145 (2015). [PubMed: 25732146]

52. Seshadri S, Faust T, Ishizuka K, Delevich K, Chung Y, Kim SH, Cowles M, Niwa M, Jaaro-Peled H, Tomoda T, Lai C, Anton ES, Li B, Sawa A, Interneuronal DISC1 regulates NRG1-ErbB4 signalling and excitatory-inhibitory synapse formation in the mature cortex. Nat Commun 6, 10118 (2015). [PubMed: 26656849]
53. Delenda C, Gaillard C, Real-time quantitative PCR for the design of lentiviral vector analytical assays. Gene Ther 12 Suppl 1, S36–50 (2005). [PubMed: 16231054]
54. Chang K, Marran K, Valentine A, Hannon GJ, Creating an miR30-based shRNA vector. Cold Spring Harb Protoc 2013, 631–635 (2013). [PubMed: 23818675]
55. de Vellis J, Cole R, Preparation of mixed glial cultures from postnatal rat brain. Methods Mol Biol 814, 49–59 (2012). [PubMed: 22144299]
56. Lee JK, Tansey MG, Microglia isolation from adult mouse brain. Methods Mol Biol 1041, 17–23 (2013). [PubMed: 23813365]
57. Ozeki Y, Pickard BS, Kano S, Malloy MP, Zeledon M, Sun DQ, Fujii K, Wakui K, Shirayama Y, Fukushima Y, Kunugi H, Hashimoto K, Muir WJ, Blackwood DH, Sawa A, A novel balanced chromosomal translocation found in subjects with schizophrenia and schizotypal personality disorder: altered l-serine level associated with disruption of PSAT1 gene expression. Neurosci Res 69, 154–160 (2011). [PubMed: 20955740]
58. Thored P, Heldmann U, Gomes-Leal W, Gisler R, Darsalia V, Taneera J, Nygren JM, Jacobsen SE, Ekdahl CT, Kokaia Z, Lindvall O, Long-term accumulation of microglia with proneurogenic phenotype concomitant with persistent neurogenesis in adult subventricular zone after stroke. Glia 57, 835–849 (2009). [PubMed: 19053043]
59. Kano S, Sato K, Morishita Y, Vollstedt S, Kim S, Bishop K, Honda K, Kubo M, Taniguchi T, The contribution of transcription factor IRF1 to the interferon-gamma-interleukin 12 signaling axis and TH1 versus TH-17 differentiation of CD4+ T cells. Nat Immunol 9, 34–41 (2008). [PubMed: 18059273]
60. Wang X, Spandidos A, Wang H, Seed B, PrimerBank: a PCR primer database for quantitative gene expression analysis, 2012 update. Nucleic Acids Res 40, D1144–1149 (2012). [PubMed: 22086960]
61. Choi VW, Asokan A, Haberman RA, McCown TJ, Samulski RJ, Production of recombinant adeno-associated viral vectors and use for in vitro and in vivo administration. Curr Protoc Neurosci Chapter 4, Unit 4 17 (2006).

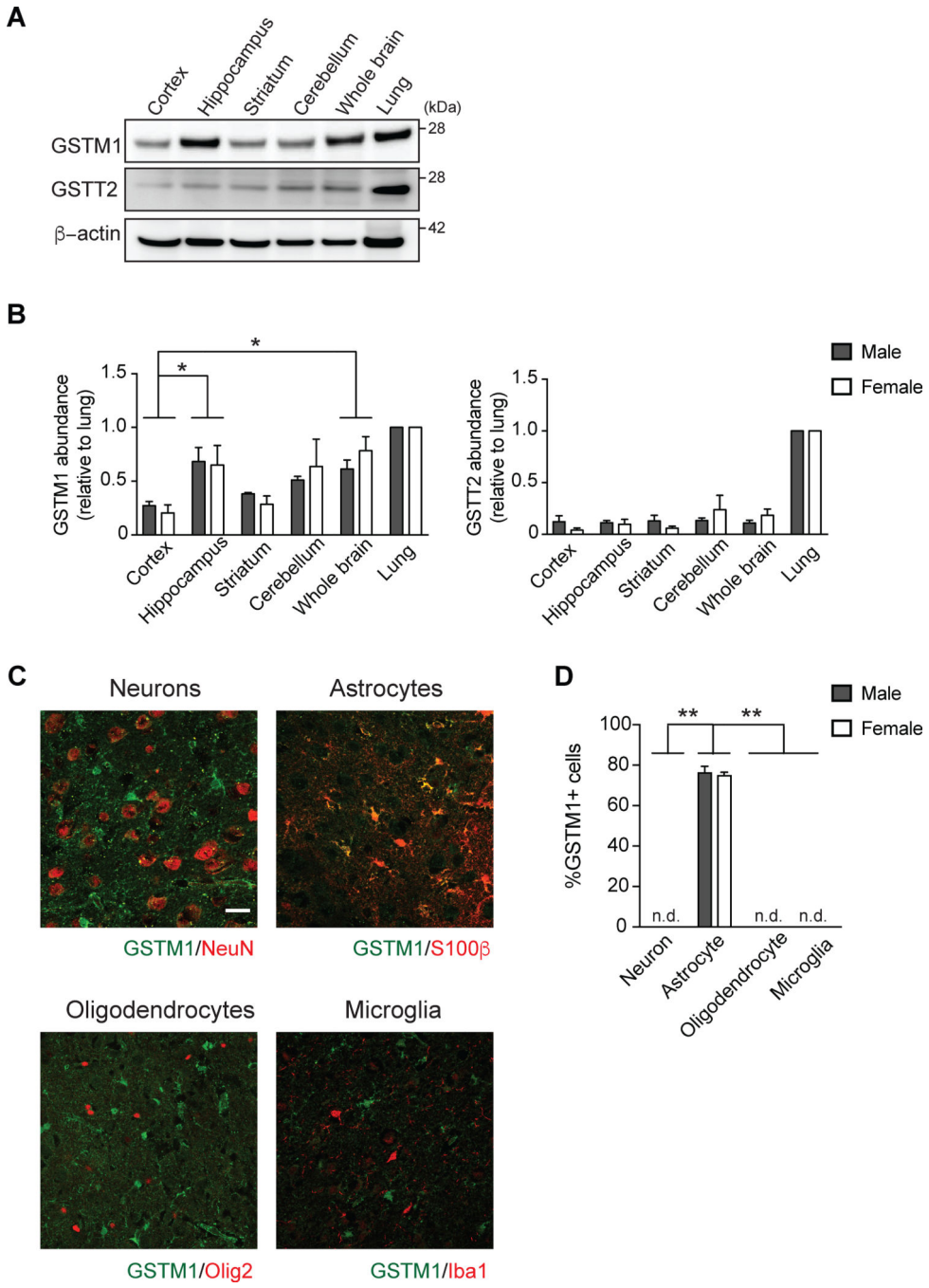

Fig. 1. Enriched expression of GSTM1 in astrocytes in the mouse brain.

(**A**) A representative Western blot for GSTM1 and GSTT2 in the cerebral cortex, hippocampus, striatum, cerebellum, whole brain, and lung of C57BL/6 WT mice (8 weeks of age, male). β-actin is a loading control. (**B**) The abundances of GSTM1 and GSTT2 in each brain area relative to that in the lung were quantified by densitometry. Male (8–11 weeks of age), n= 3 mice; Female (8 weeks of age), n = 3 mice. (**C**) Immunofluorescence showing GSTM1 in the medial prefrontal cortex (mPFC), specifically prelimbic area (PrL), in 8 weeks old C57BL/6J male mice. Cells were co-stained for cell type–specific markers to

identify neurons (NeuN), astrocytes (S100β), oligodendrocytes (Olig2), or microglia (Iba1). (**D**) Quantification of the percentage of each indicated cell type that was positive for GSTM1 staining. Male (8–11 weeks of age), n= 3 mice; Female (8 weeks of age), n = 3 mice. Scale bar, 25 μm. In (B) and (D), error bars represent mean ± SEM. *p<0.05. **p<0.01. n.d., not detected. Significance was determined by two-way ANOVA with Tukey's post-hoc test.

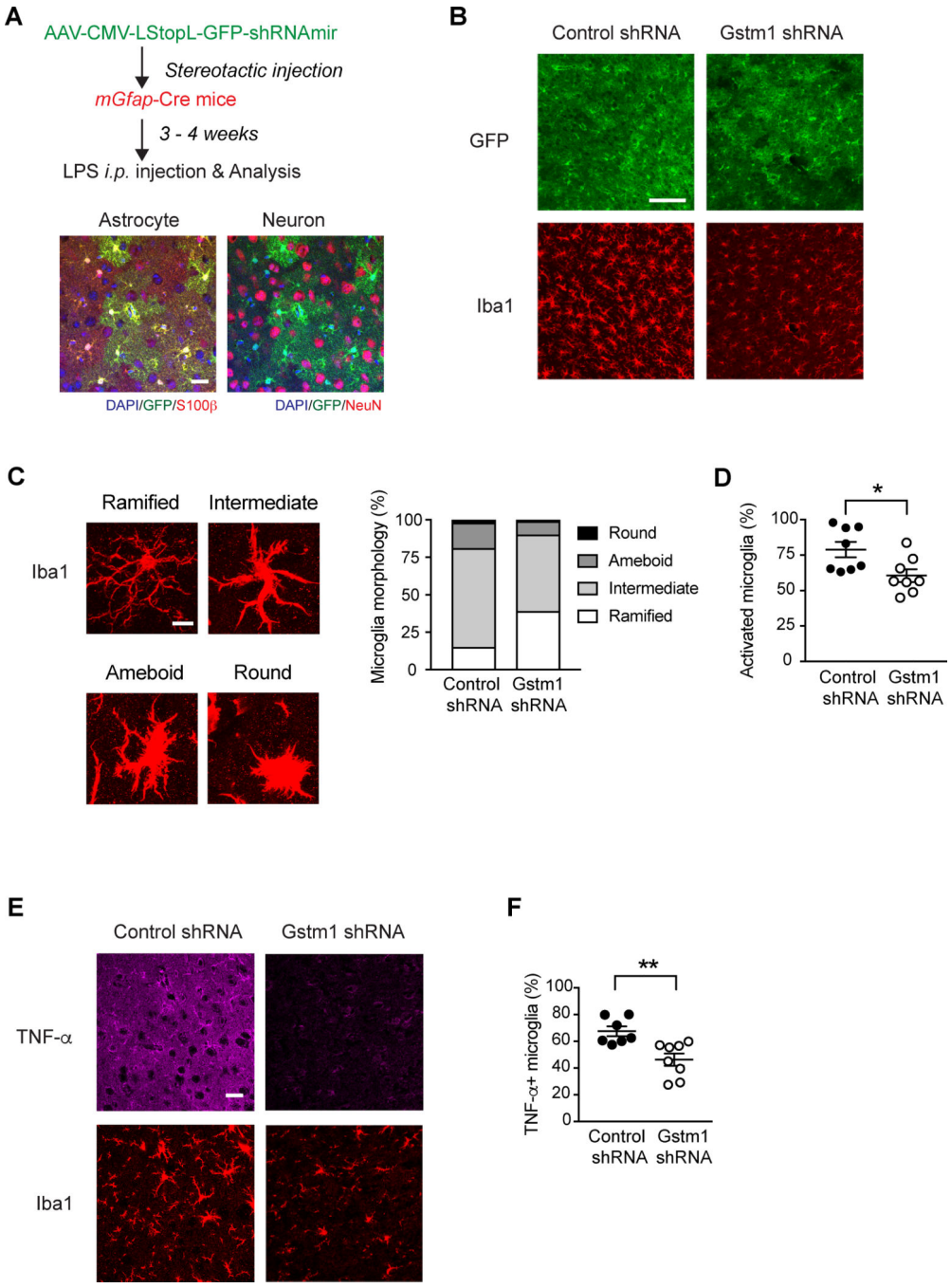

Fig. 2. Reduced activation of microglia in astrocyte-specific GSTM1 knockdown mice during brain inflammation induced by systemic injection of LPS.

(**A**) Experimental design. Mouse *Gfap* promoter–driven Cre transgenic (m*Gfap*-Cre) mice (3 weeks of age) were stereotactically injected with floxed AAV vector encoding shRNAmir against *Gstm1* (AAV-LSL-GFP-*Gstm1* shRNAmir) into the medial prefrontal cortex (mPFC) and challenged with intraperitoneal (i.p.) injection of LPS 3–4 weeks later. After 48 hours, the brains were harvested and stained for the presence of virally encoded GFP together with cell-type specific markers (NeuN for neurons and S100β for astrocytes). (**B**) Slices from the

mPFC of LPS-challenged mice injected with AAV encoding the control shRNA or *Gstm1* shRNA were stained with the microglia marker Iba1 and their activation status was analyzed by morphological changes in the area of astrocyte-specific GSTM1 knockdown (GFP^+) by confocal microscopy. (**C**) To quantify microglial activation, we morphologically classified each $Iba1^+$ microglia as ramified, intermediate, amoeboid, or round. These morphologies correspond to surveying (ramified) or activated (intermediate, amoeboid, round) microglia (58). (**D**) The microglia activation profiles were compared between the mice injected with control shRNA and those injected with *Gstm1* shRNA. n = 1,265 microglia from 8 mice for control shRNA; 941 microglia from 8 mice for *Gstm1* shRNA). (**E**) Immunofluorescence showing TNF-α in microglia in the vicinity of astrocytes with GSTM1 knockdown in mice injected with AAV encoding the control shRNA or *Gstm1* shRNA. (**F**) Quantification of the percentages of $Iba1^+$ microglia positive for TNF-α in mice in (E). n = 560 microglia from 7 mice for control shRNA; 616 microglia from 8 mice for *Gstm1* shRNA. Scale bars, 25 μm (A), 100 μm (B), 10 μm (C), and 25 μm (E). In (D) and (F), each dot represents one animal and the bar represents mean ± SEM. Significance was determined by Mann-Whitney test. $*p<0.05$, $**p<0.01$.

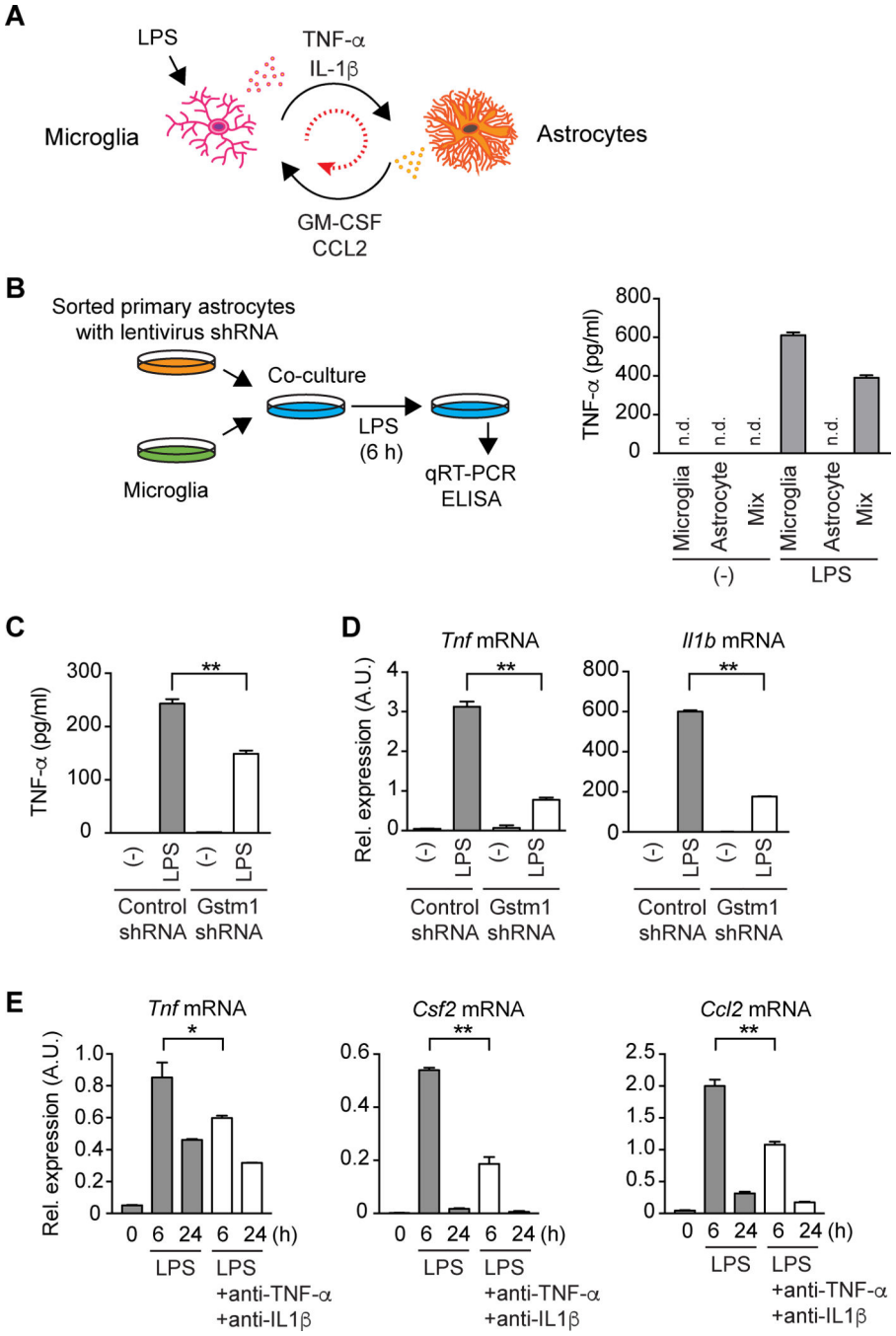

Fig. 3. Impaired production of microglial TNF-α by GSTM1 silencing in co-cultured astrocytes.

(**A**) Amplification of inflammatory responses between astrocytes and microglia through soluble mediators. Previous studies suggest that microglia produce pro-inflammatory cytokines such as TNF-α and IL-1β, which in turn stimulate astrocytes to produce pro-inflammatory mediators such as GM-CSF and CCL2, which amplify inflammatory responses in microglia. (**B**) Experimental design. Primary mouse glial cultures were prepared from 6–8 P2–5 pups (mixed male and female) and infected with lentivirus encoding shRNA. Astrocytes were enriched and then co-cultured with BV2 microglia

overnight before LPS stimulation for 6 hours. Cells and culture supernatants were harvested for qRT-PCR analysis and ELISA, respectively. The graph shows TNF-α production in response to LPS stimulation in astrocyte and microglia monocultures and in co-culture as measured by ELISA. Representative data from two biologically independent cell culture experiments were shown. (**C**) Quantification of TNF-α production in co-cultures of BV2 microglia with astrocytes expressing the control shRNA or *Gstm1* shRNA. Quantification was performed by ELISA. (**D**) Quantification of *Tnf* and *Il1b* expression in co-cultures of BV2 microglia with control or GSTM1 knockdown astrocytes. Quantification was performed by qRT-PCR of cell extracts. (**E**) Quantification of *Tnf*, *Csf2*, and *Ccl2* expression in co-cultures of BV2 microglia and WT astrocytes in the presence of TNF-α and IL-1β signaling-blocking antibodies. Quantification was performed by qRT-PCR of cell extracts. Each bar represents mean ± SD of triplicate measurements. For (C–E), representative data from three biologically independent cell culture experiments were shown. In (C) and (D), significance was determined by two-way ANOVA with Sidak's *post-hoc* test for control vs. *Gstm1* shRNA. In (E), significance was determined by one-way ANOVA with Sidak's *post-hoc* test for no-antibodies vs. anti-TNF-α/IL-1β. *$p<0.05$. **$p<0.01$. n.d., not detected. h, hours.

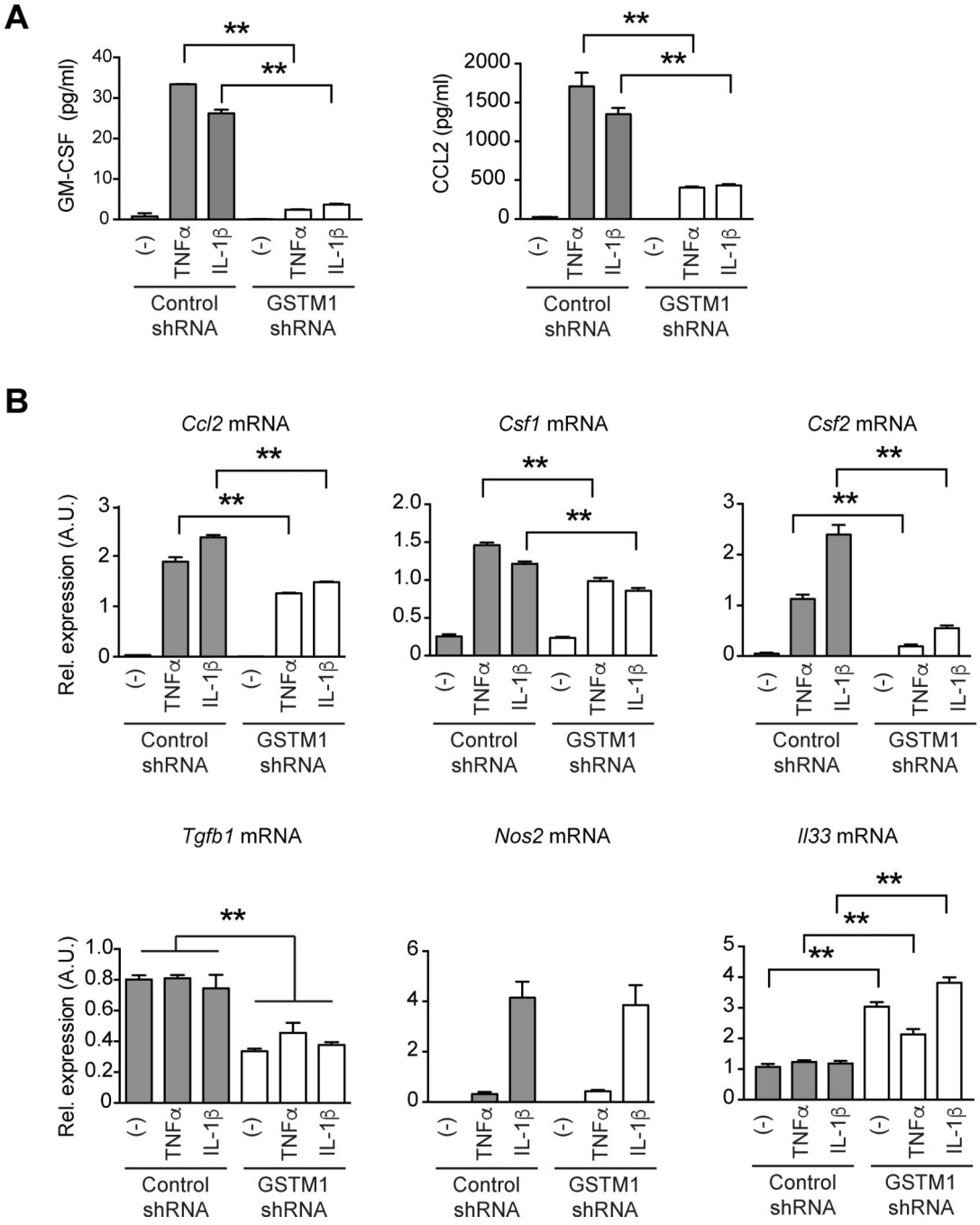

Fig. 4. Altered induction of inflammatory mediators in cultured GSTM1-knockdown astrocytes.

(**A**) Quantification of GM-CSF and CCL2 in supernatants from control and GSTM1 knockdown primary mouse cortical astrocytes in response to TNF-α and IL-1β stimulation. Quantification was performed by ELISA. (**B**) Expression of *Ccl2*, *Csf1*, *Csf2*, *Tgfb1*, *Nos2,* and *Il33* mRNAs in control and GSTM1 knockdown primary mouse cortical astrocytes stimulated with TNF-α or IL-1β. Transcripts were quantified by qRT-PCR. Each bar represents mean ± SD of triplicate measurements. Representative data from three biologically independent cell culture experiments are shown. Significance was determined

by two-way ANOVA with Sidak's *post-hoc* test for control shRNA vs. *Gstm1* shRNA. ** $p<0.01$.

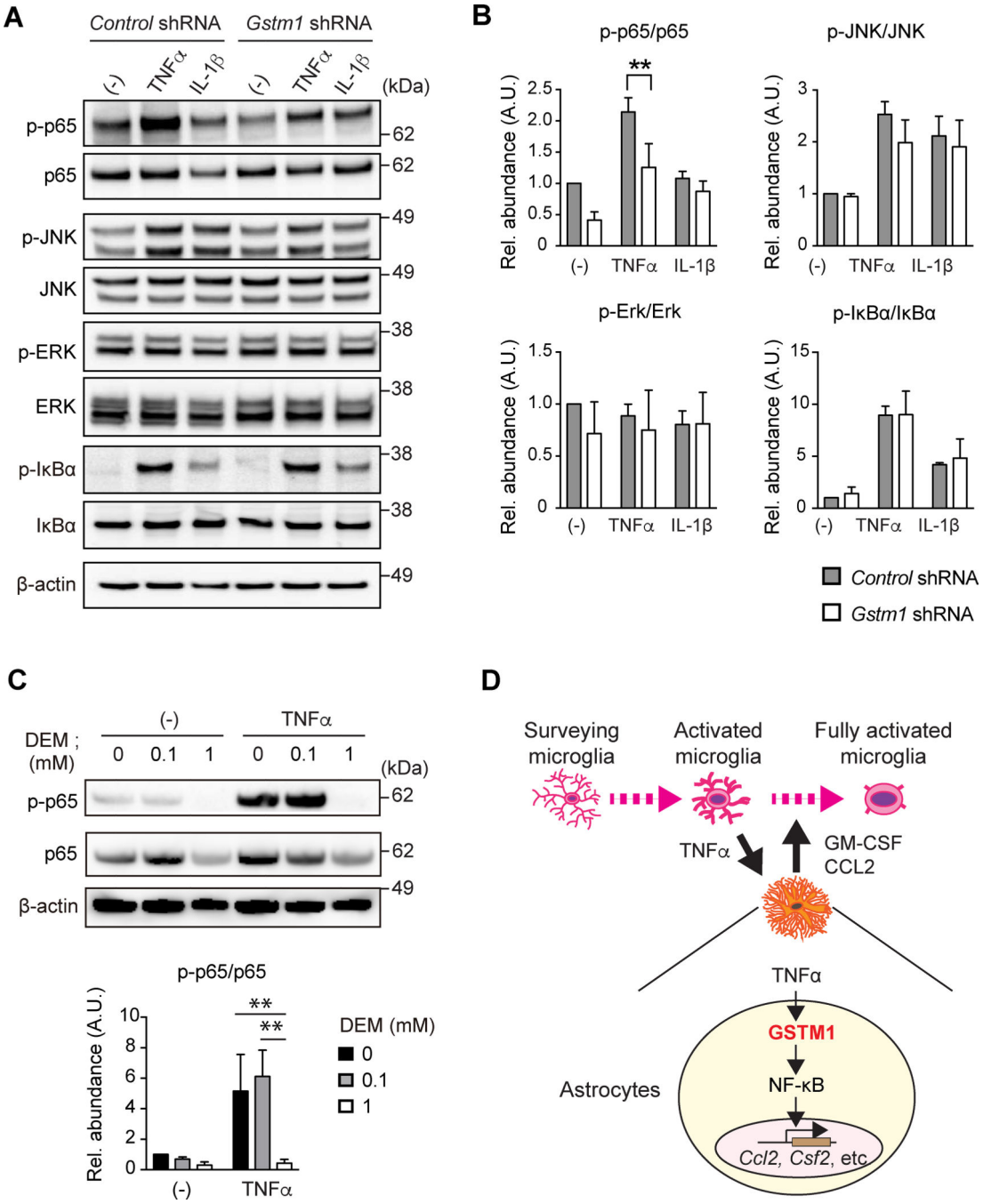

Fig. 5. GSTM1 knockdown impairs NF-κB activation in primary astrocytes.

(**A**) Western blot for the p65 subunit of NF-κB (p65), JNK, ERK, and IkBα and the phosphorylated forms of these proteins (p-p65, p-JNK, p-ERK, and p-IkBα) in primary mouse cortical astrocytes expressing a control or *Gstm1* shRNA. β-actin is a loading control. (**B**) Quantification of p65, JNK, ERK, and IkBα phosphorylation relative to the total abundance of each protein in primary mouse cortical astrocytes expressing a control or *Gstm1* shRNA. (**C**) Western blot and quantification of p65 phosphorylation in astrocytes treated with the GSH depletor DEM during TNF-α stimulation. (**D**) Schematic model of the

role of GSTM1 in astrocytes and pro-inflammatory astrocyte-microglia interactions. Our findings support the role of GSTM1 in activating NF-κB and inducing the expression of *Ccl2* and *Csf2* in astrocytes. In the absence of GSTM1, microglia activation is attenuated by insufficient amounts of astrocyte-derived GM-CSF and CCL2. This also results in a decrease in TNF-α production by microglia due to reduced positive feedback mediated by GM-CSF and CCL2. For (A) and (C), representative blot data from three independent experiments were shown. For quantification in (B) and (C), bar graphs represent mean ± SD of three biologically independent cell cultures. In (B), significance was determined by two-way ANOVA with Sidak's *post-hoc* test for control shRNA vs. *Gstm1* shRNA. In (C), significance was determined by two-way ANOVA with Tukey's *post-hoc* test. ** $p<0.01$.